2015

Comprehensive understanding of nano-sized particle separation processes using nanoparticle tracking analysis

Desmond F. Lawler

Sungmin Youn
Marshall University, youns@marshall.edu

Tongren Zhu

Ijung Kim

Boris L.T. Lau

Recommended Citation
Lawler, D. F., Youn, S., Zhu, T., Kim, I., & Lau, B. L. (2015). Comprehensive understanding of nano-sized particle separation processes using nanoparticle tracking analysis. Water Science & Technology, 72(12), 2318-2324. doi: 10.2166/wst.2015.459

Comprehensive understanding of nano-sized particle separation processes using nanoparticle tracking analysis

Desmond F. Lawler*, Sungmin Youn*, Tongren Zhu*, Ijung Kim*, and Boris L. T. Lau**

*Dept. of Civil, Architectural & Environmental Engineering, University of Texas; One University Station C1786; Austin, TX USA
dlawler@mail.utexas.edu; phone 01 512 471 4595; fax 01 512 471 0592
**Dept. of Civil & Environmental Engineering, University of Massachusetts, Amherst, MA USA

Abstract: Understanding of nano-sized particle separation processes has been limited by difficulties of nanoparticle characterization. In this study, nanoparticle tracking analysis (NTA) was deployed to evaluate the absolute particle size distributions in laboratory scale flocculation and filtration experiments with silver nanoparticles. The results from NTA were consistent with standard theories of particle destabilization and transport. Direct observations of changes in absolute particle size distributions from NTA enhance both qualitative and quantitative understanding of particle separation processes of nano-sized particles.
Keywords: particle size distribution; flocculation; granular media filtration; silver nanoparticles

Introduction

Characterizing the size distribution of nanoparticles is essential to understanding particle separation processes. Dynamic light scattering (DLS) and electron microscopy (EM) are used most frequently, despite their limitations in obtaining particle size distributions (Malloy and Carr, 2006). Nanoparticle tracking analysis (NTA), a relatively new analytical technique, overcomes these difficulties by direct laser microscopy observation of Brownian motion of each particle, and then derives particle sizes using the Stokes-Einstein equation (Gallego-Urrea *et al.*, 2011). In this study, flocculation and filtration of silver nanoparticles (AgNPs) were investigated using the Nanosight NTA instrument (Nanosight, UK) to monitor the changes in particle size distributions.

Materials and Methods

Chemicals. Spherical citrate-capped AgNPs and polyvinylpyrrolidone (PVP)-capped AgNPs with diameters of 50 nm were purchased (Nanocomposix, USA). Calcium nitrate ($Ca(NO_3)_2$), sodium nitrate ($NaNO_3$), and magnesium nitrate ($Mg(NO_3)_2$) were used to control the ionic strength, and the pH was kept constant at 7.0(±0.3) via sodium bicarbonate (0.1 mmol/L $NaHCO_3$). Suwannee River humic acid and fulvic acid (International Humic Substances Soc., MN) were used as natural organic matter (NOM). Laboratory glassware was cleaned by soaking in 10% nitric acid overnight and kept in a particle-free room prior to each experiment.

Nanosight NTA. In this study, particle size distributions of AgNPs were measured exclusively using Nanosight LM10 HS equipped with software version NTA 2.3. This instrument uses laser illuminated microscopy to record the Brownian motion of nanoparticles in suspension. NTA 2.3 is a computer program that tracks each particle from the recorded videos, calculates the particles' mean squared displacements, and from that information and the Stokes-Einstein equation, the particles' diffusion coefficients and sphere-equivalent radius. The method and theory of NTA are described by Malloy and Carr (2006). The lower size limit of detection depends on the refractive index (RI) of nanoparticles and, for colloidal silver, is approximately 10 nm (Carr *et al.*, 2008; Filipe, *et al.*, 2010). For this research, each measurement was taken for sixty seconds and run in triplicate. The average values of three measurements were used for the analysis. Although the software allows fitting the data to a log-normal distribution, the raw data were used in the analysis for two reasons. First, the absolute, and not just relative, size distributions reflect the changes brought about by flocculation and filtration more precisely; these processes promote heterodispersity in the distribution, and a log-normal model fitting would distort the actual data. Second, NTA 2.3 classifies particles in equal arithmetic increments of size, but it is better in process analysis to use equal logarithmic increments (Benjamin and Lawler, 2013). Therefore, the raw data were used to produce particle size distributions with equally spaced size increments on a logarithmic scale.

Flocculation. For the flocculation experiments, the stock suspension of AgNPs (1 mg/mL) was diluted to a concentration of 500 μg/L. The $Ca(NO_3)_2$ or $NaNO_3$ stock solution was added at time 0 to achieve desired ionic strengths and rapidly mixed for 30 seconds. Samples were collected at various times (0, 15, 30, 45, 60, and 120 minutes) and particle size distributions were measured immediately. Throughout each flocculation experiment, gentle mixing (with G values estimated as 10 s^{-1}) was applied via a combined rocking and rolling motion in enclosed jars to avoid particle settling. Flocculation experiments were performed by varying three different independent variables (capping agents of AgNPs, ionic strengths of the two electrolytes, and initial nanoparticle concentrations) while other environmental conditions were fixed. The conditions for each flocculation experiment are shown in Table 1.

Table 1. Experimental conditions for flocculation

Experiment Number	Capping Agent	Ionic Strength (mM)	Electrolyte	Initial Concentration (μg/L)
1	Citrate	2	$Ca(NO_3)_2$	500
2	Citrate	10	$Ca(NO_3)_2$	500
3	Citrate	2	$Na(NO_3)$	500
4	Citrate	10	$Na(NO_3)$	500
5	PVP	2	$Ca(NO_3)_2$	500
6	PVP	10	$Ca(NO_3)_2$	500
7	Citrate	10	$Ca(NO_3)_2$	250
8	Citrate	10	$Ca(NO_3)_2$	125

Filtration. The filtration setup and operation were identical to the previously reported conditions (Lawler *et al.*, 2013). The 3.8 i.d. cylindrical column was packed with 325 μm glass beads to a depth of 10 cm. Background solution and AgNPs suspension were pumped separately at a ratio of 20:1 and mixed at the top to yield an influent concentration of 100 μg/L and a filtration velocity of 2 m/h. The column tests were performed under different ionic strengths with different electrolytes ($Ca(NO_3)_2$, $NaNO_3$, and $Mg(NO_3)_2$), and a few experiments were performed with 3.5 mg/L TOC (humic acid and fulvic acid). Filtration conditions are shown in Table 2; all experiments were performed with citrate-capped AgNPs. Prior to time zero, the column was flushed with DI water and then background solution for 30 minutes. The filtration was then conducted in three 30-minute phases: AgNPs suspension, background electrolyte solution, and DI water. The effluent was sampled at various times (7, 17 and 27 minutes) for immediate particle size distribution measurement with the Nanosight instrument; the times were chosen to yield sufficient time to allow one measurement to be completed before the next sample was taken and to see if there was any time trend. The effluent was also collected every one to two minutes for total silver mass concentration measurement by inductively coupled plasma-optical emission spectrometer (ICP-OES, Varian 710-ES) after 3% nitric acid dissolution.

Table 2. Experimental conditions for filtration

Experiment Number	Ionic Strength (mM)	Electrolyte	NOM
1	1	$Ca(NO_3)_2$	No
2	5	$Ca(NO_3)_2$	No
3	10	$Ca(NO_3)_2$	No
4	10	$Ca(NO_3)_2$	Humic acid
5	10	$Ca(NO_3)_2$	Fulvic acid
6	10	$Mg(NO_3)_2$	No
7	10	$NaNO_3$	No
8	100	$NaNO_3$	No

Results and Discussion

Flocculation experiments. Figure 1 shows the changes in the absolute particle size distributions over two hours of flocculation at the different ionic strengths achieved by $Ca(NO_3)_2$ (Expts. 1 and 2). At I = 2 mM (Figure 1A), essentially no change in the size distribution (i.e., no flocculation) occurred. At I = 10 mM (Figure 1B), the peak of the number distribution shifted to larger particles, both the height of the peak number concentration and the area of the figure (total particle concentration) lowered with time, and the creation of larger flocs is clearly indicated. These results are clear evidence of flocculation and are at least qualitatively consistent with the Smoluchowki theory of flocculation, i.e., many small particles aggregated to form fewer larger particles.

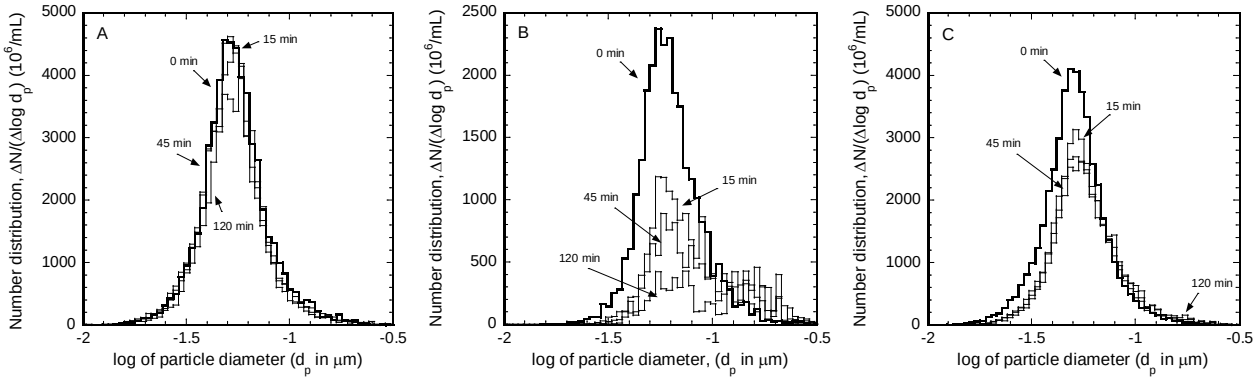

Figure 1. Flocculation: Number distribution citrate-capped AgNPs at ionic strengths of (A) 2 mM with $Ca(NO_3)_2$ (B) 10 mM with $Ca(NO_3)_2$ and (C) 10mM with $NaNO_3$ (Data from 30 and 60 minutes omitted to reduce clutter.)

Identical experiments were performed with $NaNO_3$ in lieu of $Ca(NO_3)_2$ at the same ionic strengths of 2 and 10 mM (Expts. 3 and 4). Consistent with the results of Expt. 1, the number distribution did not change over two hours of flocculation when the ionic strength was at 2 mM (not shown), but at I = 10 mM (Figure 1C), changes in particle sizes were observed. The peak of the number distribution shifted slightly to the right while the height of the peak and the area of number distribution lowered with time. These results confirmed that flocculation occurred but the degree of flocculation was not nearly as significant as in Expt. 2 with $Ca(NO_3)_2$ (Figure 1B). The difference in the degree of flocculation between Expts. 2 and 4 ($Ca(NO_3)_2$ vs. $NaNO_3$ at I = 10 mM) was previously described based on the surface chemistry (Lawler *et al.*, 2013). Calcium ion has a higher affinity than sodium ion to form complexes with citrate (Morel & Hering, 1993), and the surface charge of citrate-capped AgNPs is more effectively neutralized by $Ca(NO_3)_2$ than $NaNO_3$ according to the zeta potential determination. That is, $Ca(NO_3)_2$ destabilizes citrate-capped AgNPs by adsorption and charge neutralization as well as by compression of the double layer, whereas $NaNO_3$ only uses the latter mechanism.

When PVP-capped AgNPs were used for the identical flocculation experiment at the ionic strengths of 2 and 10 mM of $Ca(NO_3)_2$ (Expts. 5 and 6, shown in Figure 2), the destabilization was only by double layer compression, so the results are similar to those for $NaNO_3$ destabilization of citrate-capped AgNPs (Figure 1C).

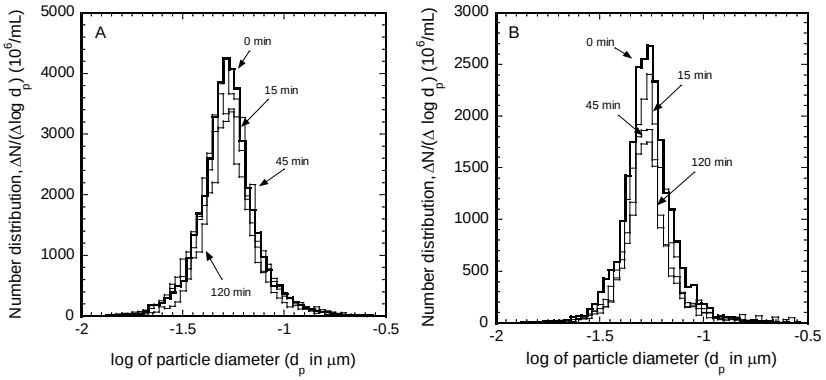

Figure 2. Number distribution of PVP-capped AgNPs at ionic strengths of (A) 2mM and (B) 10mM with $Ca(NO_3)_2$

The value of NTA measurements is clear when compared with DLS results (Malvern Zetasizer) from a similar experiment for citrate-capped AgNPs at the ionic strength of 10 mM of $Ca(NO_3)_2$, as shown in Figure 3. DLS does indicate flocculation by the shift to larger sizes but only gives relative size measurements (area under all curves is one) and creates a Gaussian distribution to fit the ensemble light scattering detected; this result is not consistent with Smoluchowski principles.

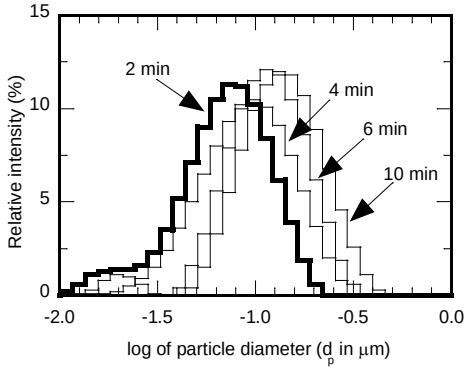

Figure 3. Number distribution at ionic strengths 10mM $Ca(NO_3)_2$ from Dynamic Light Scattering

Flocculation experiments were also performed using initial concentrations of citrate-capped AgNPs reduced by factors of two (Expt. 7) and four (Expt. 8) from Expt. 2; all other parameters remained fixed. Because flocculation is a second order reaction with respect to the particle number concentration, the initial concentration dictates reaction kinetics (Benjamin and Lawler, 2013). The results from Expts. 7 and 8 resembled the previous result from Expt. 2 in the indicators of flocculation. The influence of the initial concentration on flocculation kinetics can be readily seen by comparing some characteristic changes in the size distributions among the three experiments. Figure 4 shows changes in the number fractions (*i.e.*, the ratio of the number concentration of particles in particular diameter ranges to the total number concentration). Two particle diameter ranges, equally spaced logarithmically, were chosen as the "smaller particle range" ($-1.5 < \log(d_p) < -1.0$, or $31.6\ \text{nm} < d_p < 100\ \text{nm}$) and "larger particle range" ($-1.0 < \log(d_p) < -0.5$, or $100\ \text{nm} < d_p < 316\ \text{nm}$). During flocculation, the fraction of smaller particles decreased while the fraction of the larger particles increased. At time 0, the smaller particles accounted for more than 90% of the total number of AgNPs. At the initial concentration of 500 μg/L (Expt. 2, Figure 4A), the fraction of smaller particles decreased to nearly 50% during two hours of flocculation whereas the number of larger particles increased to nearly 50%. These trends were less dramatic in the experiments with lower initial concentrations of AgNPs (Figure 4B and C). The smaller particle fractions were approximately 60% and 80% at the end of flocculation when the initial concentrations were 250, and 125 μg/L, respectively. These results are consistent with the Smoluchowski principle that flocculation kinetics depend on the initial number concentration of particles.

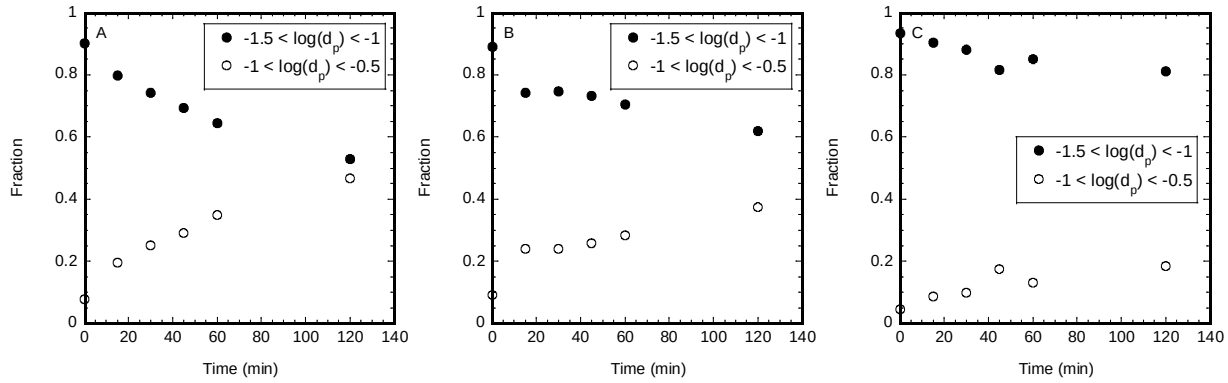

Figure 4. Flocculation: Particle number fractions at (A) 500, (B) 250, and (C) 125 µg/L

Filtration experiments. Figure 5 shows the changes in the absolute particle size distributions through filtration at the different ionic strengths achieved by $Ca(NO_3)_2$ and $NaNO_3$. At I = 1 mM with $Ca(NO_3)_2$ (Fig 5A), almost no AgNPs removal was achieved by the filter and essentially no change in the size distribution occurred. At I = 10 mM (Figure 5B), almost complete removal was achieved by the filter as very few particles are seen in the effluent. Some aggregation of particles inside the filter was also observed: the effluent had a greater number of larger particles than the influent. The same trend of increasing removal efficiency with increasing ionic strength was also observed in the experiments with $NaNO_3$ as the electrolyte. The observation of greater attachment at higher ionic strength suggests that electrostatic repulsion between the approaching particles and the filter media surface is decreased by reduced double layer thickness at higher ionic strength (Lin *et al.*, 2011). The appearance of larger particles under high ionic strength suggests some aggregation of particles inside the filter. However, the hydraulic detention time through the packed media is only one minute, not long enough for substantial aggregation between particles in the influent at this concentration. It is more likely that the large particles in the effluent are evidence that aggregation takes place when approaching particles in the influent collide with and attach to previously attached particles on the surface of filter media and subsequently detach together.

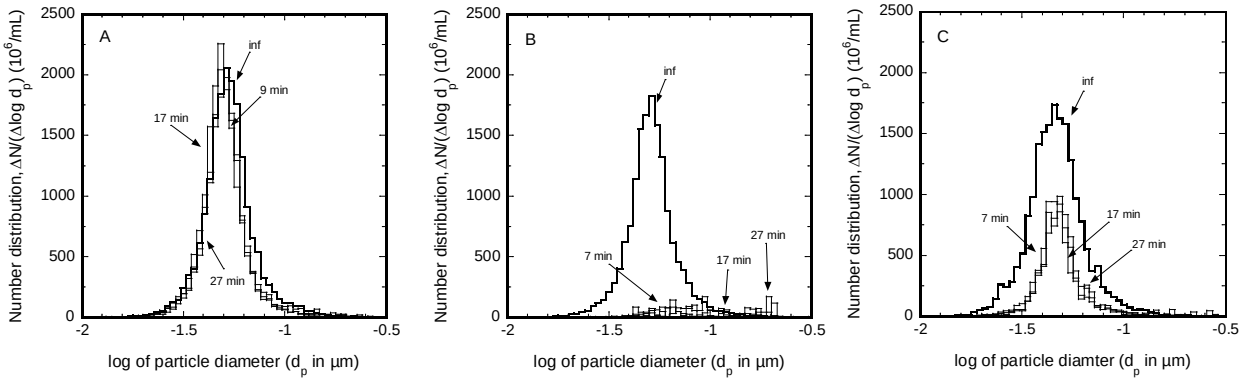

Figure 5. Number distribution of citrate-capped AgNPs through filtration at ionic strength of (A) 1 mM with $Ca(NO_3)_2$, (B) 10 mM with $Ca(NO_3)_2$, and (C) 10 mM with $NaNO_3$

Effects of different electrolytes on citrate-coated AgNPs deposition are shown by comparing Figures 5B and 5C. At I = 10 mM, almost complete removal was achieved by the filter when $Ca(NO_3)_2$ was the source of ionic strength (Figure 5B), but much less removal was achieved when $NaNO_3$ was used as background electrolyte (Figure 5C). As in the flocculation experiments, the difference is ascribed to the complexation of Ca^{2+} with the citrate on the surface of these AgNPs; similar results were observed with Mg^{2+} as the electrolyte as Mg^{2+} has almost identical stability constants for citrate complexation as Ca^{2+} (Morel and Hering, 1993). Both Ca^{2+} and Mg^{2+} lead to charge neutralization and reduction of zeta potential of the citrate-AgNPs and thus reduce the electrostatic repulsion between the filter media and the particles (Badawy *et al.*, 2010).

Figure 6 shows the influence of NOM on deposition of citrate-AgNPs at I = 10 mM with $Ca(NO_3)_2$. In the absence of NOM (Figure 6A), citrate-AgNPs attached strongly to the filter media, and removal efficiency was very high. However, the presence of humic acid (Figure 6B) hindered deposition and reduced the attachment of particles onto the collector surface. Ca^{2+} is known to complex with carboxyl groups in humic acid, and thus the contribution of Ca^{2+} to deposition was reduced in the presence of humic acid (Badawy *et al.*, 2010). In addition, the association of humic acid with polymer coating of AgNPs probably reduced the active sites on the particle surface that could attach to the filter media (Yang, *et al.*, 2014). In contrast to the humic acid results, the presence of fulvic acid (Figure 6C) did not greatly lower the removal efficiency; this result is consistent with the work of Furman *et al*. (2013) who found that humic acid bound itself to AgNP surfaces more successfully than fulvic acid, so that humic acid led to less aggregation and deposition.

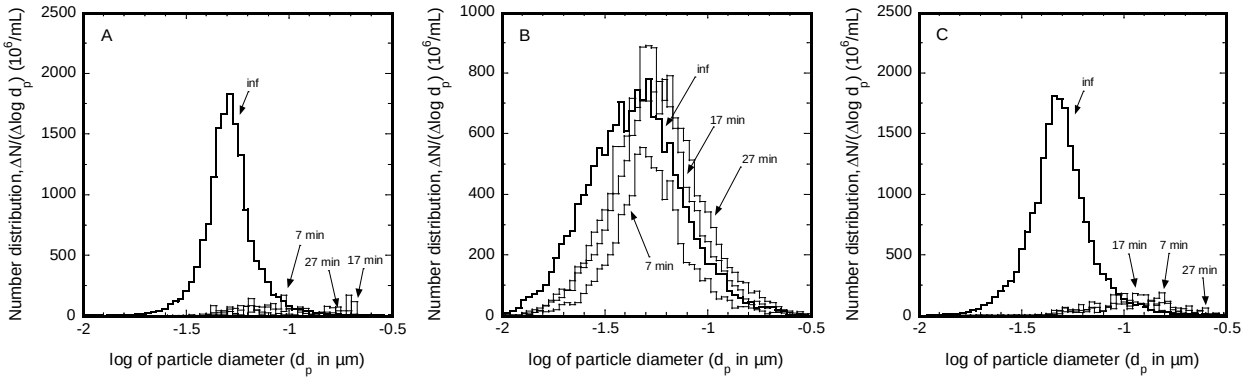

Figure 6. Number distribution of citrate-capped AgNPs through filtration at ionic strength of 10 mM with $Ca(NO_3)_2$ (A) without NOM, (B) with humic acid and (C) with fulvic acid.

Results of particle removal on a number basis from NTA were also compared with results of the mass measurements by ICP-OES. In most cases, results from the two measurements were quite consistent. This agreement again indicates that NTA could be a promising method to characterize nanoparticles during treatment processes both qualitatively and quantitatively. However, the number and size information from the NTA were translated into particle volume information (assuming spherical particles), and the agreement with the ICP-OES measurements with the volume remaining was not nearly so good, especially when the number fraction remaining was low. This result suggests that the size of flocs is overestimated by the NTA or that the fractal dimension of the flocs was not accounted for in the volume calculation.

Conclusions

The changes in absolute particle size distributions in the nanoparticle range during flocculation and filtration processes were detailed using nanoparticle tracking analysis (NTA). The experimental results with different independent variables are compatible with standard theories of particle destabilization, and the particle size changes are consistent with the Smoluchowski theory of flocculation. The NTA results are also in good agreement with the theory of particle transport in porous media, and measurements from NTA were consistent with other analytical tools such as ICP-OES but provided far greater detail.

Although the primary interest in this research was to monitor the changes in particle size distributions in both flocculation and filtration, the destabilization results are also remarkable. For the citrate-capped AgNPs, destabilization with calcium or magnesium nitrate was for more effective than using the same ionic strength solution of sodium nitrate; both calcium and magnesium form complexes with citrate, so the mechanism of destabilization with these ions was charge neutralization, whereas it was only compression of the double layer with sodium. For PVP-coated AgNPs, the electrolytes were indifferent and the only destabilization was accomplished by double

layer compression. Only two filtration experiments were performed with natural organic matter; citrate-capped AgNPs were used with 10 mM $Ca(NO_3)_2$, conditions that caused optimal destabilization and removal without the NOM. In the presence of humic acid, particle deposition was greatly reduced while fulvic acid did not cause much hindrance to deposition.

Acknowledgements. This work was funded by the Nasser I. Al-Rashid Chair in Civil Engineering, the endowed chair held by author Desmond Lawler.

References

Badawy, A. M. E., Luxton, T. P., Silva, R. G., Scheckel, K. G., Suidan, M. T., and Tolaymat, T. M. 2010 Impact of environmental conditions (pH, ionic strength, and electrolyte type) on the surface charge and aggregation of silver nanoparticles suspensions. *Env. Sci. & Tech.*, **44**(4), 1260-1266.

Benjamin, M. M., and Lawler, D. F. 2013 *Water quality engineering: physical/chemical treatment processes*. John Wiley & Sons. Hoboken, New Jersey.

Carr, R., Hole, P., Malloy, A., Smith, J., Weld, A., and Warren, J. 2008 The real-time, simultaneous analysis of nanoparticle size, zeta potential, count, asymmetry and fluorescence. *Nanotech, **1***, 866-870.

Filipe, V., Hawe, A., and Jiskoot, W. 2010 Critical evaluation of Nanoparticle Tracking Analysis (NTA) by NanoSight for the measurement of nanoparticles and protein aggregates. *Pharmaceutical Research*, **27**(5), 796-810.

Furman, O, Usenko, S., and Lau, B.L.T. 2013 Relative Importance of the Humic and Fulvic Fractions of Natural Organic Matter in the Aggregation and Deposition of Silver Nanoparticles, *Env.Sci.&Tech.*, **47**, 1349-1356.

Gallego-Urrea, J. A., Tuoriniemi, J., and Hassellöv, M. 2011 Applications of particle-tracking analysis to the determination of size distributions and concentrations of nanoparticles in environmental, biological and food samples. *Trends in Analytical Chemistry*, **30**(3), 473-483.

Lawler, D. F., Kim, I., Mikelonis, A. M., Lau, B., and Youn, S. 2013 Silver nanoparticle removal from drinking water: flocculation/sedimentation or filtration? *Water Science & Technology: Water Supply*, **13**(5), 1181-1187.

Lin, S., Cheng, Y., Bobcombe, Y., L. Jones, K., Liu, J., and Wiesner, M. R. 2011 Deposition of silver nanoparticles in geochemically heterogeneous porous media: predicting affinity from surface composition analysis. *Env. Sci. & Tech.*, **45**(12), 5209-5215.

Malloy, A. and Carr, B. 2006 NanoParticle Tracking Analysis – The Halo™ System. *Particle & Particle Systems Characterization*, **23**(2): 197–204.

Morel, F.M.M., and Hering, J.G. 1993 *Principles and Applications of Aquatic Chemistry*, John Wiley & Sons, New York.

Yang, X, Lin, S, and Wiesner, M. R. 2014 Influence of natural organic matter on transport and retention of polymer coated silver nanoparticles in porous media. *J. of Hazardous Materials*. **264**, 161-168.